Complement C3 and C3aR mediate different aspects of emotional behaviours; relevance to risk for psychiatric disorder

Laura J. Westacott[1,4†], Trevor Humby[1,2†], Niels Haan[1], Sophie A. Brain[2], Emma-Louise Bush[2], Margarita Toneva[7], Andreea-Ingrid Baloc[2], Anna L. Moon[1], Jack Reddaway[1,4], Michael J. Owen[1,] Jeremy Hall[1,4], Timothy R. Hughes[3,4], B. Paul Morgan[3,4,6], William P. Gray[1,4,5$] & Lawrence S. Wilkinson[1,2,4*$]

[1] Neuroscience and Mental Health Research Institute, MRC Centre for Neuropsychiatric Genetic and Genomics, School of Medicine, Hadyn Ellis Building, Cardiff University, Cardiff, CF24 4HQ, UK.[2] Behavioural Genetics Group, Schools of Psychology and Medicine, Cardiff University, Cardiff, CF10 3AT, UK. [3] Complement Biology Group, Systems Immunity Research Institute, School of Medicine, Cardiff University, CF14 4XW, Cardiff UK. [4] Hodge Centre for Neuropsychiatric Immunology, School of Medicine, Cardiff University, Cardiff CF24 4HQ, UK. [5] Brain Repair and Intracranial Therapeutics (BRAIN) Unit, School of Medicine, Cardiff University, CF24 4HQ, UK. [6] UK Dementia Research Institute, Cardiff University, Cardiff, CF24 4HQ, UK. [7] Institute of Psychiatry, Psychology and Neuroscience, King's College London, London, SE5 8AF, UK.

[†] These authors contributed equally to the work
[$]Joint senior authors: Lawrence S. Wilkinson & William P. Gray

[*]Corresponding author: Lawrence S. Wilkinson

Email address: WilkinsonL@cardiff.ac.uk

Address: Neuroscience and Mental Health Research Institute, School of Medicine, Cardiff University, Cardiff, CF24 4HQ, UK

Key words: *Complement system, Anxiety, Fear, Stress response.*

Abstract

Complement is a key component of the immune system with roles in inflammation and host-defence. Here we reveal novel functions of complement pathways impacting on emotional reactivity of potential relevance to the emerging links between complement and risk for psychiatric disorder. We used mouse models to assess the effects of manipulating components of the complement system on emotionality. Mice lacking the complement C3a Receptor (*C3aR*$^{-/-}$) demonstrated a selective increase in unconditioned (innate) anxiety whilst mice deficient in the central complement component C3 (*C3*$^{-/-}$) showed a selective increase in conditioned (learned) fear. The dissociable behavioural phenotypes were linked to different signalling mechanisms. Effects on innate anxiety were independent of C3a, the canonical ligand for C3aR, consistent with the existence of an alternative ligand mediating innate anxiety, whereas effects on learned fear were due to loss of iC3b/CR3 signalling. Our findings show that specific elements of the complement system and associated signalling pathways contribute differentially to heightened states of anxiety and fear commonly seen in psychopathology.

1. Introduction

The complement system is a key component of the immune system that plays a pivotal role in inflammation and host-defence. Complement activation occurs via several pathways, all of which lead to cleavage of the central protein, C3 (see Figure S1). Activation of C3 generates the fragments C3a and C3b. C3a is an anaphylatoxin that signals via its canonical G-protein coupled receptor C3aR[1]. Activation of this receptor has been demonstrated to trigger calcium mobilization[2-4], stimulating an array of intracellular signalling pathways to induce both pro- and anti-inflammatory effects[1,5]. C3b on the other hand propagates further complement activation by contributing to the cleavage of complement component 5 (C5) downstream of C3 and, after further cleavage to iC3b, plays a role in opsonisation by macrophages and microglia via complement receptor 3 (CR3). Akin to C3, C5 cleavage generates C5a (another anaphylatoxin and a ligand for the C5a receptor, C5aR) and C5b, which triggers the terminal complement pathway by sequentially binding proteins C6, C7, C8 and C9. These proteins subsequently congregate to assemble the membrane attack complex (MAC) which ultimately results in destruction of the target cell or pathogen via cell lysis[6].

In the central nervous system evidence is emerging that complement has functions beyond its canonical immune roles[7]. Neurons, astrocytes and microglia express complement receptors and regulators, and are also capable of synthesising complement proteins[8,9]. The expression patterns of these vary over the course of brain development[10]. Complement impacts a number of neurodevelopmental processes including neurogenesis[11], migration[12] and synaptic elimination[13] as well as ongoing synaptic plasticity processes underlying learning and memory in the adult brain[14].

Furthermore, there is increasing evidence that complement is causally involved in the pathogenesis of neurodegenerative and psychiatric conditions. In Alzheimer's disease, genetic variants in complement related loci have been associated with increased disease risk[15,16], and complement knockout mice exhibit reduced age-related synapse loss[17] and neuropathology[18]. Alterations in complement proteins and activation have also been reported in sera from individuals with autism-spectrum disorder[19] schizophrenia[20], major depressive disorder[21], bipolar disorder[22] and post-traumatic stress disorder[23]. In the case of schizophrenia, an important finding comes from elegant genetic work demonstrating that structural variation in the complement *C4A* locus is associated with risk of developing the disease[24]. C4 cleavage generates fragments that contribute to the activation of C3, yielding C3a and C3b. Given the known roles for the iC3b/CR3 pathway in developmental synaptic pruning[13,25], it has been suggested that *C4A* variants may impact on psychiatric risk via this mechanism, with excessive synaptic elimination leading to abnormal connectivity and disruption of neural networks[24]. Variants in *C3* and putative complement-control genes *CSMD1* and *CSMD2* have also been implicated in genetic susceptibility for schizophrenia[26,27].

Altered emotional function, in particular maladaptive anxiety and fear, is a pervasive and clinically important symptom in schizophrenia and a frequent comorbidity across several of the DSM-5 and ICD-11 defined disorders. Anxiety and fear exist along a spectrum of aversive emotional states and can be elicited by differing environmental factors to result in distinguishable behavioural outputs[28]. Anxiety is characterised by sustained arousal, hypervigilance and risk assessment surrounding anticipated or potential threats, while fear is often characterised as an acute response to an experienced, imminent danger resulting in immediate avoidance, fight or freezing

behaviour[29,30]. Whilst there is significant overlap in the neurocircuitry underlying these states, there are also contributions from distinct neuronal circuitries[28,31].

There is previous data suggesting complement may play a role in emotional responses to aversive circumstances. Mice overexpressing the human *C4A* variant associated with risk for schizophrenia demonstrated elevated anxiety behaviour[32]. Anxiety phenotypes have also been reported in mice exposed to excessive pre-natal complement activity[33] and neurodegeneration-associated anxiety phenotypes are reduced by complement inhibitors[34]. Furthermore, aged *C3* deficient mice exhibited lower levels of anxiety alongside enhanced learned fear responses[17], whereas increased anxiety has been reported in mice lacking the C3aR[35]. These previous studies suggest that complement can influence both innate and learned aversive behaviours, however, the precise complement signaling pathways responsible for effects on these dissociable aspects of emotionality is unknown.

Utilising the central role of C3 in complement signalling, we used a combination of complement knockout mice to functionally parse innate anxiety and learned fear related phenotypes. In homozygous *C3* knockout mice (*C3*$^{-/-}$)[36] complement cannot be activated beyond C3, and therefore these animals lack C3 activation fragments (C3a, C3b) and downstream activation products (C5a, C5b) and thus cannot activate the terminal complement pathway. Phenotypes in this model could therefore be the result of loss of any of these downstream effector molecules. We compared the *C3*$^{-/-}$ model with homozygous *C3aR* knockout mice (*C3aR*$^{-/-}$)[37]. In these mice, complement is intact apart from the capacity for C3a to bind its canonical receptor C3aR and hence through use of both models, we tested the extent to which phenotypic effects were the

result specifically of disrupted C3a/C3aR signalling. A priori, because C3a is an obligate cleavage fragment of C3, we hypothesised that any phenotypes dependent on interaction of C3a and C3aR would be apparent in both *C3*$^{-/-}$ and *C3aR*$^{-/-}$ models.

2. Materials and Methods

2.1 Mouse models and husbandry. Wildtype and *C3*$^{-/-}$ strains were sourced in-house from Professor B. Paul Morgan and Dr Timothy Hughes (strains originally from The Jackson Laboratory; B6.PL-Thy1^{a}/CyJ stock#000406 and B6;129S4-C3tm1Crr/J stock#003641 respectively); *C3aR*$^{-/-}$ mice were provided by Professor Craig Gerard of Boston Children's Hospital, USA (strain subsequently provided to The Jackson Laboratory; B6.129S4(C)- *C3ar1*^{tm1Cge}/BalouJ; stock#033904). *C5*$^{-/-}$ mice (as described in [38]) were provided by Professor Marina Botto, Imperial College London. This strain originated from naturally C5-deficient DBA/2J mice, that had been backcrossed to C57Bl/6J. *C3*$^{-/-}$, *C3aR*$^{-/-}$ and *C5*$^{-/-}$ strains were maintained via homozygous x homozygous breeding and were on a C57Bl/6J background. In all experiments, knockout mice were compared to wildtype mice also on a C57Bl/6J background. Mice were between 3-8 months old during experimental testing and were kept in a temperature and humidity-controlled vivarium (21±2°C and 50±10%, respectively) with a 12-hour light-dark cycle (lights on at 07:00hrs/lights off at 19:00hrs). Home cages were environmentally enriched with cardboard tubes, soft wood blocks and nesting materials and animals were housed in single sex littermate groups (2-5 mice/cage). Standard laboratory chow and water were available *ad libitum*. All procedures were performed in accordance with the requirements of the UK Animals (Scientific Procedures) Act (1986).

2.2 General behavioural methods. Testing took place between the hours of 09:00 and 17:00, with random distribution of testing for subjects of different genotypes throughout the day. Mice were habituated to the test rooms for 30 min prior to testing. All assays involved individual testing of mice and apparatus was cleaned thoroughly with a 70% ethanol solution between subjects.

2.3 Data collection. Data for the elevated plus maze, elevated zero maze and open field were collected using EthoVision XT software (Noldus Information Technology, Netherlands) via a video camera mounted above the centre of each piece of apparatus. Tracking of each subject was determined as the location of the greater body-proportion (12 frames/s) in the specific virtual zones of each piece of apparatus.

2.4 The elevated plus maze (EPM). The maze, positioned 300 mm above the floor and illuminated evenly at 15 lux, was constructed of opaque white Perspex and consisted of two exposed open arms (175 x 78 mm^2, length x width, no ledges) and two equally sized enclosed arms, which had 150 mm high walls[39]. Equivalent arms were arranged opposite one another. Subjects were placed at the enclosed end of a closed arm and allowed to freely explore for 5 minutes. Data from each pair of arms were combined to generate single open and closed arm values (number and duration of arm entries and latency of first entry to each arm). In addition, the following parameters were manually scored (by an experimenter positioned at a computer in the same room as the maze, watching the live-video stream of the test); number of stretch-attend postures (SAPs; defined as the animal slowly and carefully reaching towards the open arms in a low, elongated body posture[40,41]) and number of head dips from the open arms (looking down over the edge of an open arm).

2.5 The elevated zero maze (EZM). The maze, positioned 520 mm above the floor and illuminated evenly at 15 lux, was constructed of wood and consisted of two exposed open regions (without ledges; 52 mm wide) and two equally sized enclosed regions (also 52 mm wide), which had 200 mm high grey opaque walls. The diameter of the maze was 600mm. Equivalent regions were arranged opposite one another. Subjects were placed at the border of one of the open and closed regions and allowed to freely explore for 5 min. Data from each pair of regions were combined to generate single open and closed region values (number and duration of region entries and latency of first entry to each region). In addition, the number of head dips (as above) were measured. Due to the high walls of the enclosed sections of the maze, subjects were not visible to the experimenter when in the closed regions and therefore these parameters were scored only when a subject was on the open regions.

2.6 Locomotor activity (LMA). LMA was measured in an apparatus consisting of twelve transparent Perspex chambers (each 210 x 360 x 200 mm, width x length x height). Two infrared beams were embedded within the walls of each chamber, which crossed the chamber 30 mm from each end and 10 mm from the chamber floor. Individual subjects were placed in a designated chamber for a 120 min duration on three consecutive days. Beam breaks were recorded as an index of activity, using a computer running custom written BBC Basic V6 programme with additional interfacing by ARACHNID (Cambridge Cognition Ltd, Cambridge, UK). Data were analysed as the total number of beam breaks per session per day.

2.7 Fear-potentiated startle (FPS). FPS was assessed using startle chamber apparatus which consisted of a pair of ventilated and soundproofed SR-LAB startle chambers (San Diego Instruments, CA, USA) each containing a non-restrictive Plexiglas cylinder (35 mm in diameter), mounted on a Perspex plinth, into which a subject was placed. The motor responses of subjects to white noise stimuli (generated from a speaker 120 mm above the cylinder) were recorded via a piezoelectric accelerometer, attached centrally below the Plexiglas cylinder, which converted flexion plinth vibration into electrical signals. The peak startle response, within 200ms from the onset of each startle presentation, in each trial, was normalized for body weight differences using Kleiber's 0.75 mass exponent[42] as per[43]. A computer running SR-Lab software (Version 94.1.7.48) was used to programme trials and record data. A foot shock grid connected to a shock generator (San Diego Instruments, CA, USA) was inserted into the Plexiglas cylinder before conditioning sessions.

FPS consisted of three separate sessions presented over a two-day period (see Figure 4A). On the first day, mice were given a pre-conditioning session immediately followed by the conditioning session. The pre-conditioning session started with a 5 min acclimatisation phase followed by presentation of 3 no-stimulus trials, and then a block of pulse-alone trials presented at 90, 100 and 110dB (5 of each at 40 ms duration). Trials were randomly distributed throughout the session and presented with a 60 s random interval (range 36 s to 88 s). After the pre-conditioning session was complete, mice were removed from the startle chambers, restraint tubes cleaned, and shock grids were placed into the Plexiglas cylinders prior to commencing the conditioning session. The mice were then returned to the startle chambers and subjected to a session consisting of a 5 min acclimatisation phase followed by 3 CS+shock trials, with

3 no stimulus trials before and after, presented with a 2min random interval (range 1.5 to 3min). The scrambled 0.14 mA, 0.5 s foot shock was delivered in the final 0.5 s of the 30 s visual CS. Following a 24hr delay, subjects were assessed for FPS in the post-conditioning session. This session followed the same format as the pre-conditioning session (5 min acclimatisation phase followed by presentation of 3 no-stimulus trials, and then a block of pulse-alone trials presented at 90, 100 and 110dB, with 5 of each at 40 ms duration) however the final block of trials also included pulse+CS trials at 90, 100 and 110 dB (5 of each), with the startle pulse presented in the final 40 ms of the CS. FPS was determined as the fold change between pulse-alone trials and pulse+CS trials within the post-conditioning session.

2.8 Corticosterone measurements. Testing took place between the hours of 10:00 and 14:00 to account for the diurnal pattern of corticosterone release[44]. Mice were allowed to freely explore the EPM for 5 min, after which they were placed in a holding cage for a further 25 min before being culled by cervical dislocation. Control mice were removed from their home cage and immediately culled. There was an equal distribution of subjects of different genotypes, counterbalanced between the two test conditions and throughout the testing period. Trunk blood was collected into heparin tubes (Becton Dickinson, USA) and immediately centrifuged at 4000 rpm for 10 min, and the supernatant removed and frozen at -80°c until further use. A corticosterone ELISA was performed according to manufacturer's instructions (ADI-900-097, Enzo Life Sciences, UK) and analysed using a four-parameter logistic curve plug in (https://www.myassays.com/four-parameter-logistic-curve.assay).

2.9 Diazepam study. Wildtype, *C3*$^{-/-}$ and *C3aR*$^{-/-}$ were used and were randomly assigned to either vehicle or drug conditions within each genotype. A three-day dosing regimen of diazepam (2 mg/kg, i.p., Hameln Pharmaceuticals, UK) or an equivalent volume of vehicle (0.1 M phosphate buffered saline, pH 7.4) was used, based on pilot testing in wildtype mice to establish an effective anxiolytic dose with minimal sedative effects (data not included). Following 2 days of pre-treatment, diazepam or vehicle was administered 30 min prior to testing on the EPM on the 3rd day.

2.10 Tissue for gene expression analysis. Mice were removed from their home cage and immediately culled via cervical dislocation. Brains were removed and the following regions dissected: medial prefrontal cortex (mPFC), ventral hippocampus (vHPC) and cerebellum (see Figure 6A) and frozen at -80° until further use.

2.11 Quantitative Polymerase Chain Reaction (qPCR). Gene expression was analysed using standardised qPCR methods with quantification using the $2^{-\Delta\Delta Ct}$ method[45]. Brain tissue from the mPFC, vHPC and the cerebellum was analysed. RNA was extracted using the RNeasy kit (QIAGEN) and was subsequently treated with DNAse to remove genomic DNA (TURBO DNA-free kit, Thermo Fisher Scientific). RNA was then converted to cDNA (RNA to cDNA EcoDry Premix, Random Hexamers, Clontech, Takara). cDNA samples were run in triplicate in 96 well reaction plates using SYBR-Green-based qPCR (SensiFast, HI-ROX, Bioline) according to manufacturer's instructions using a StepOnePlus System (Applied Biosystems, Thermo Fisher Scientific). Genotypes were counterbalanced across plates and genes of interest were run alongside housekeeping genes *Gapdh* and *Hrpt1* for each sample, within the same reaction plate. All samples were run in triplicate and samples differing by >0.3 Cts

were excluded. The change in expression of genes of interest, after normalisation to the two house-keeping genes (ΔCt) was transformed to yield $2^{-\Delta\Delta Ct}$ values. Relative changes from wildtype animals were calculated for each gene of interest.

2.12 Primers. Primers were designed to span at least one exon-exon junction and to match the target sequence only in mouse (Primer-Blast, NCBI) and were synthesised commercially (Sigma Aldrich). Primer efficiency was determined separately through a dilution series of cDNA samples from wildtype hippocampus, cerebellum and cortex. Primers with an efficiency between 90-110% were selected.

Table 1. List of primer sequences used.

Gene	Species	Forward	Reverse
Gapdh	Mouse	GAACATCATCCCTGCATCCA	CCAGTGAGCTTCCCGTTCA
Hprt1	Mouse	TTGCTCGAGATGTCATGAAGGA	AATGTAATCCAGCAGGTCAGCAA
Gabra2	Mouse	AAGCCACTGGAGGAAAACATCT	TTAGCCAGCACCAACCTGAC
Crhr1	Mouse	CTTCAACTCTTTCCTGGAGTCCT	TGGCAGAGCGGACCTCA
Nr3c1	Mouse	AAACTCTGCCTGGTGTGCTC	GGTAATTGTGCTGTCCTTCCAC
Cacna1c	Mouse	ATGGTTCTTGTCAGCATGTTGCGG	TGCAAATGTGGAACCGGTAAGTG
Cacna1d	Mouse	AGAGGACCATGCGAACGAG	CCTTCACCAGAAATAGGGAGTCT
Cacna1e	Mouse	CTCATGTCACCACCGCTAGG	TCTGTCTGCACCACCTTTGG

2.13 Genotyping Genotyping was performed on post-mortem tail tip samples. Qiagen DNeasy Blood and Tissue Kits (Qiagen, Manchester, UK) were used to extract genomic DNA (gDNA) as per the manufacturers standard protocol. For *C3*$^{-/-}$ mice, JAX protocol 27746 was used (common; ATCTTGAGTGCACCAAGCC, wildtype; GGTTGCAGCAGTCTATGAAGG, mutant; GCCAGAGGCCACTTGTATAG) and for

C3aR$^{-/-}$ JAX protocol 27638 was used (common; AGCCATTCTAGGGGCGTATT, wild type reverse; CATGGTTTGGGGTTATTTCG, mutant reverse; TTGATGTGGAATGTGTGCGAG). For both genotypes, a touchdown cycling protocol was used (see JAX protocols for details). Genotyping for *C5*$^{-/-}$ mice was performed as described in [38].

2.14 Statistical analysis. All statistical analyses were carried out using GraphPad Prism 8.4.1 (GraphPad Software, CA, USA). Data was assessed for equality of variances using the Brown-Forsythe test and then appropriate parametric (*t* test, one-way or two-way ANOVA) or non-parametric (Kruskal-Wallis) tests used. *Post hoc* pairwise comparisons were performed using the Tukey or Dunn's tests for parametric or non-parametric analyses, respectively. For all analyses, alpha was set to 0.05 and exact p values were reported unless $p<0.0001$. All p values were multiplicity adjusted[46]. Data are expressed as mean ± standard error of the mean.

The main between-subjects' factor for all ANOVA analyses was GENOTYPE (WT, *C3*$^{-/-}$, *C3aR*$^{-/-}$, or *C5*$^{-/-}$). For the EPM, LMA and FPS experiments, there were within-subject factors of ZONE (open, closed, middle), DAY (1,2,3) and STIMULUS INTENSITY (90, 100, 110 dB) respectively. Analysis of plasma corticosterone by two-way ANOVA included an additional between subject factor of CONDITION (baseline, EPM), and for the diazepam experiment, there was an additional between subject factor of DRUG (diazepam, vehicle). For qPCR analyses, ΔCt values were analysed by one-way ANOVA.

3. Results

3.1 Increased innate anxiety in *C3aR*$^{-/-}$ but not *C3* $^{-/-}$ mice. Using a cohort of male wildtype, *C3*$^{-/-}$ and *C3aR*$^{-/-}$ mice we first assessed emotional reactivity in the elevated plus maze (EPM), a well-established test of innate anxiety in rodents which exploits the conflict between the drive to explore novel environments and the innate aversion towards open, brightly lit spaces[47,48]. Heatmaps indexing overall maze exploration over a 5-minute session demonstrated major differences in open arm exploration between genotypes (Figure 1A; see Supplementary Video 1 for representative examples). Notably, in comparison to wildtype and *C3*$^{-/-}$ mice, *C3aR*$^{-/-}$ mice took significantly longer to first enter the open arms (Figure 1B) and spent less time on the open arm per entry (Figure S2A), leading to a reduced overall duration spent in the open arms (Figure 1C), findings consistent with increased anxiety. The ethological parameters head dips and stretch attend postures (SAPs) also differed between genotypes (Figure 1D,E), with *C3aR*$^{-/-}$ mice exhibiting decreases in the former and increases in the latter, a pattern of results again consistent with heightened anxiety[49]. We also noted a significantly increased frequency of head dipping in *C3*$^{-/-}$ mice (Figure 1D), suggestive of reduced levels of anxiety relative to both wildtype and *C3aR*$^{-/-}$ mice[50].

These initial data were consistent with an anxiogenic phenotype present in *C3aR*$^{-/-}$ mice but absent in *C3*$^{-/-}$ mice. We confirmed the findings in two further independent tests of anxiety using additional cohorts of animals. First we used the elevated zero maze (EZM, see Methods Section 2.6), another test of anxiety-like behaviour which similarly probes behavioural responses to exposed, illuminated spaces[51]. The data

recapitulated the pattern of findings seen in the EPM (Figure 1F-J). Additional data from the open field test, where *C3aR*$^{-/-}$ mice were more likely to avoid the centre of the arena, were also consistent in demonstrating a specific anxiety-like phenotype in *C3aR*$^{-/-}$ but not *C3*$^{-/-}$ mice (Figure S3). Given that several of the measures indexing anxiety were dependent on movement around the apparatus it was important to eliminate potential locomotor confounds. To address this issue, we measured activity independently in a non-anxiety provoking environment and found no differences in locomotor activity between genotypes (Figure S2C), demonstrating that anxiety measures were unlikely to be influenced by movement confounds. Importantly, experiments conducted in female mice demonstrated comparable *C3aR*$^{-/-}$ anxiety phenotypes in both the elevated plus maze and open field (Figure S6&7).

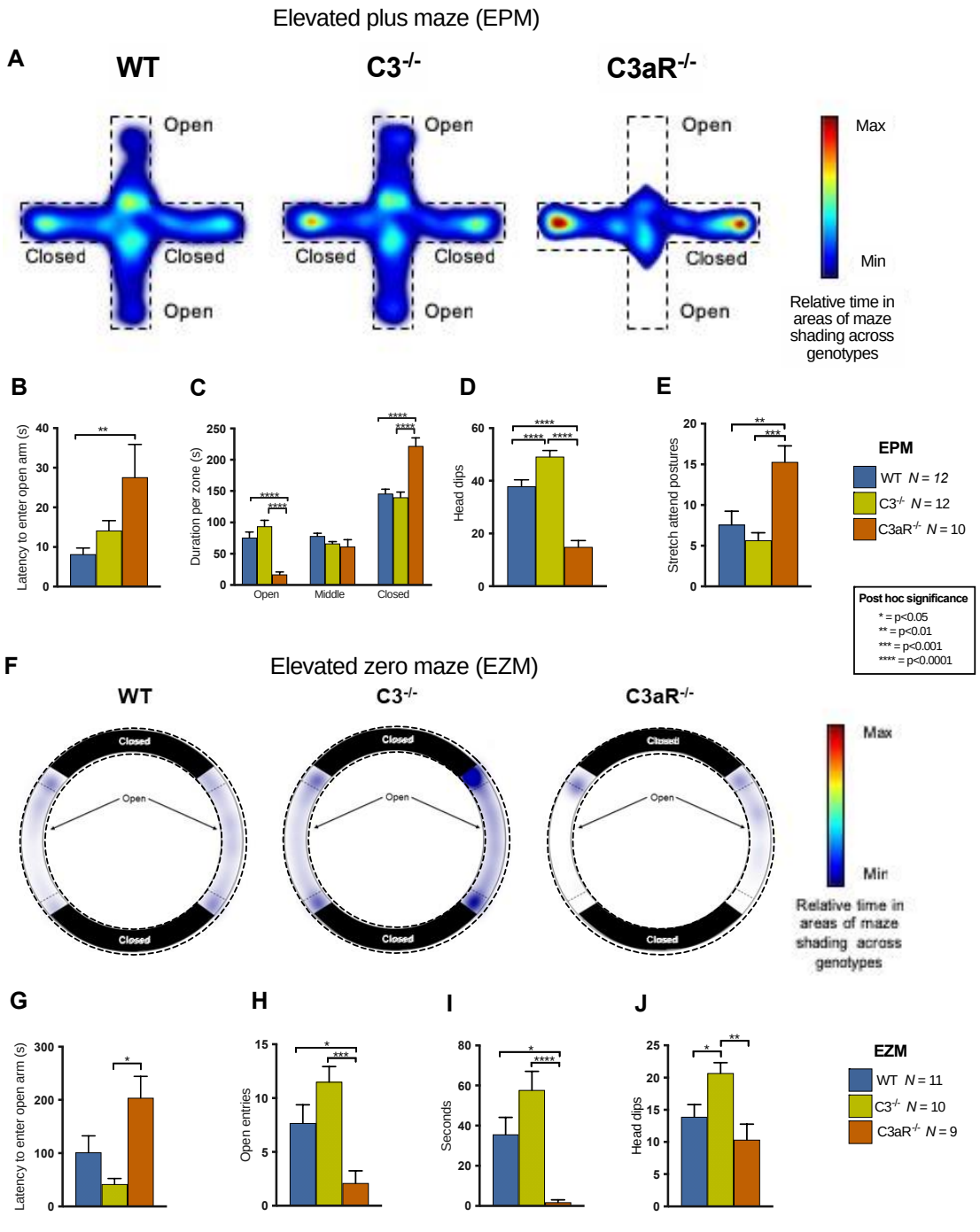

Figure 1. *C3aR*$^{-/-}$, but not *C3*$^{-/-}$ mice show increased anxiety-like behaviour in the elevated plus maze (EPM;A-E) and elevated zero maze (EZM;F-J). (A) Heatmaps displaying relative time per zone of the EPM across genotypes **(B)** Latency to first open arm visit; wildtype 8.21±1.53s, *C3*$^{-/-}$ 14.1±2.52s, *C3aR*$^{-/-}$ 27.6±8.31s, (H_2=10.5, p=0.005). *Post hoc* tests demonstrated that *C3aR*$^{-/-}$ mice took significantly longer to first enter the open arms than wildtype mice (p=0.0045). **(C)** *C3aR*$^{-/-}$ mice distributed

their time across the EPM differently to wildtype and *C3*$^{-/-}$ mice (GENOTYPE×ZONE, $F_{4,62}$=17.7, p=0.0001) spending less time in the open arms (*C3aR*$^{-/-}$ 16.70±3.73s vs. wildtype 75.78±8.86s, p<0.0001, *C3aR*$^{-/-}$ vs. *C3*$^{-/-}$ 93.86±9.59s p<0.0001) and significantly more time in the closed arms (*C3aR*$^{-/-}$ 221.88±12.06s vs. wildtype 146.01±7.01s, p<0.0001, and *C3*$^{-/-}$ 140.04±8.61s p<0.0001). **(D)** *C3aR*$^{-/-}$ (14.90±2.22) mice performed significantly fewer head dips than wildtype (37.92±2.53, p<0.0001) and *C3*$^{-/-}$ mice (49.17±2.37, p<0.0001), whereas *C3*$^{-/-}$ mice performed significantly more head dips than wildtype mice (p=0.0061; overall ANOVA $F_{2,31}$=48.0, p<0.0001). **(E)** *C3aR*$^{-/-}$ mice performed significantly more stretch attend postures (SAPs; 15.30±1.80) than wildtype (7.58±1.66, p=0.0042) and *C3*$^{-/-}$ mice (5.67±0.94, p=0.0004; overall ANOVA $F_{2,31}$=10.3, p=0.0004). **(F)** Heatmaps displaying relative exploration of the open segments of the elevated zero maze, across genotypes. Note that due to the height of the walls in the closed regions it was not possible to track mice or observe ethological behaviours such as grooming or SAPs. **(G)** There was a significant difference in the latency to first enter the open arms (wildtype 101.00±31.00s, *C3*$^{-/-}$ 42.00±2.52s, *C3aR*$^{-/-}$ 204.00±40.40s, H_2=8.13, p=0.0171). *Post hoc* tests revealed that *C3aR*$^{-/-}$ mice took significantly longer than *C3*$^{-/-}$ mice to initially enter the open region (p=0.0140). **(H)** The number of entries made to open regions differed between genotypes (wildtype 7.69±1.69, *C3*$^{-/-}$ 11.5±1.43s, *C3aR*$^{-/-}$ 2.10±1.15, $F_{2,30}$=8.96, p=0.0009). *C3aR*$^{-/-}$ mice made significantly fewer entries to the open areas than wildtype (p=0.0324) and *C3*$^{-/-}$ mice (p=0.0006) and **(I)** spent significantly less time on the open arms (1.77±1.29) compared to wildtype (35.7±8.43s, p=0.0132) and *C3*$^{-/-}$ (57.7±9.32s, p<0.0001; overall Kruskal-Wallis test H_2=19.2, p<0.0001). **(J)** *C3*$^{-/-}$ mice performed significantly more head dips (20.7±1.62) than wildtype (13.9±1.89,

p=0.048) and *C3aR*$^{-/-}$ mice (10.3±2.42, p=0.0034; overall ANOVA $F_{2,27}$=6.86,p=0.0039). Data are mean ± S.E.M. *, **, *** and **** represent p≤0.05, p≤0.01, p≤0.001 and p≤0.0001 for *post-hoc* genotype comparisons, respectively.

3.2 Neuroendocrine response in *C3aR*$^{-/-}$ and *C3*$^{-/-}$ mice following exposure to the elevated plus maze

We next tested whether the behavioural measures of anxiety were paralleled by changes in plasma levels of the stress hormone corticosterone. In a separate cohort of wildtype, *C3*$^{-/-}$ and *C3aR*$^{-/-}$ male mice, we assayed plasma corticosterone 30 minutes after exposure to the EPM and compared levels to those of a group of animals who remained in their home-cages. There were no genotype differences in basal corticosterone levels; however, being placed on the EPM increased plasma corticosterone 6-15-fold in all genotypes, demonstrating that the EPM was a potent stressor (Figure 2A). *Post hoc* analyses showed a significantly greater EPM-evoked corticosterone response in the *C3aR*$^{-/-}$ animals, consistent with their increased anxiety-like behaviour observed on the maze.

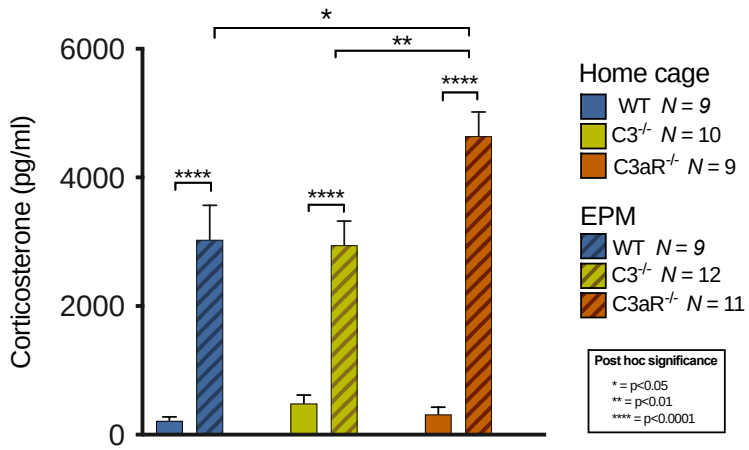

Figure 2. Neuroendocrine response following exposure to the elevated plus maze (A) 5-minute exposure to the EPM significantly elevated corticosterone in all genotypes (main effect of CONDITION, $F_{1,54}$=143, p<0.0001; baseline 344.66±63.70 vs. EPM 3553.84±274.13). There was a significant GENOTYPE × CONDITION interaction ($F_{2,54}$=4.64, p=0.0138). *Post hoc* analysis showed that after the EPM, *C3aR*$^{-/-}$ mice demonstrated significantly higher corticosterone levels (4640.27±376.13) than wildtype (3033.78±535.06, p=0.0127) and *C3*$^{-/-}$ mice (2948.00±374.87, p=0.0032). *Post hoc* tests also indicated that there were no baseline differences between genotypes (wildtype 216.54±63.2 vs. *C3aR*$^{-/-}$ 316.17±111.60 p>0.9999, wildtype vs. *C3*$^{-/-}$ p=0.9927, and *C3*$^{-/-}$ 485.60±130.35 vs.*C3aR*$^{-/-}$ mice p=0.9992). Data represent mean + S.E.M. *, **, and **** represent p≤0.05, p≤0.01 and p≤0.0001 for *post-hoc* genotype comparisons, respectively.

3.3 Altered sensitivity of *C3aR*$^{-/-}$ and *C3*$^{-/-}$ mice to diazepam in the elevated plus maze

In a further independent cohort of male mice, we tested the sensitivity of EPM induced anxiety-like behaviour to the benzodiazepine diazepam, an established clinically effective anxiolytic drug[47,52]. Our initial behavioural findings were replicated in vehicle-treated animals across all behavioural indices of anxiety, again showing an anxiogenic phenotype in *C3aR*$^{-/-}$ but not *C3*$^{-/-}$ mice (Figure 3A). As anticipated, in wildtype mice 2mg/kg diazepam led to a trend for increased time on the open arms (Figure 3B) and a significant reduction in SAPs which are considered to reflect risk assessment behaviour[53-55](Figure 3C). These effects were therefore consistent with reduced anxiety[50,55]. In contrast, the same dose of drug that was effective in eliciting anxiolysis

in wildtypes was without effects in *C3aR*$^{-/-}$ mice (Figure 3A,B,C) and produced a seemingly anxiogenic (increased anxiety) pattern of effects in *C3*$^{-/-}$ mice (Figure 3A,B and Figure S4B,C). Locomotor activity monitored across all the maze (Figure S4D) indicated that wildtype and *C3aR*$^{-/-}$ mice were unlikely to have been influenced by diazepam-induced sedation. In *C3*$^{-/-}$ mice however, activity was significantly suppressed under drug conditions indicating a possible sedative effect. Together, these data indicated a fundamentally altered reactivity to diazepam in both *C3*$^{-/-}$ and *C3aR*$^{-/-}$ models.

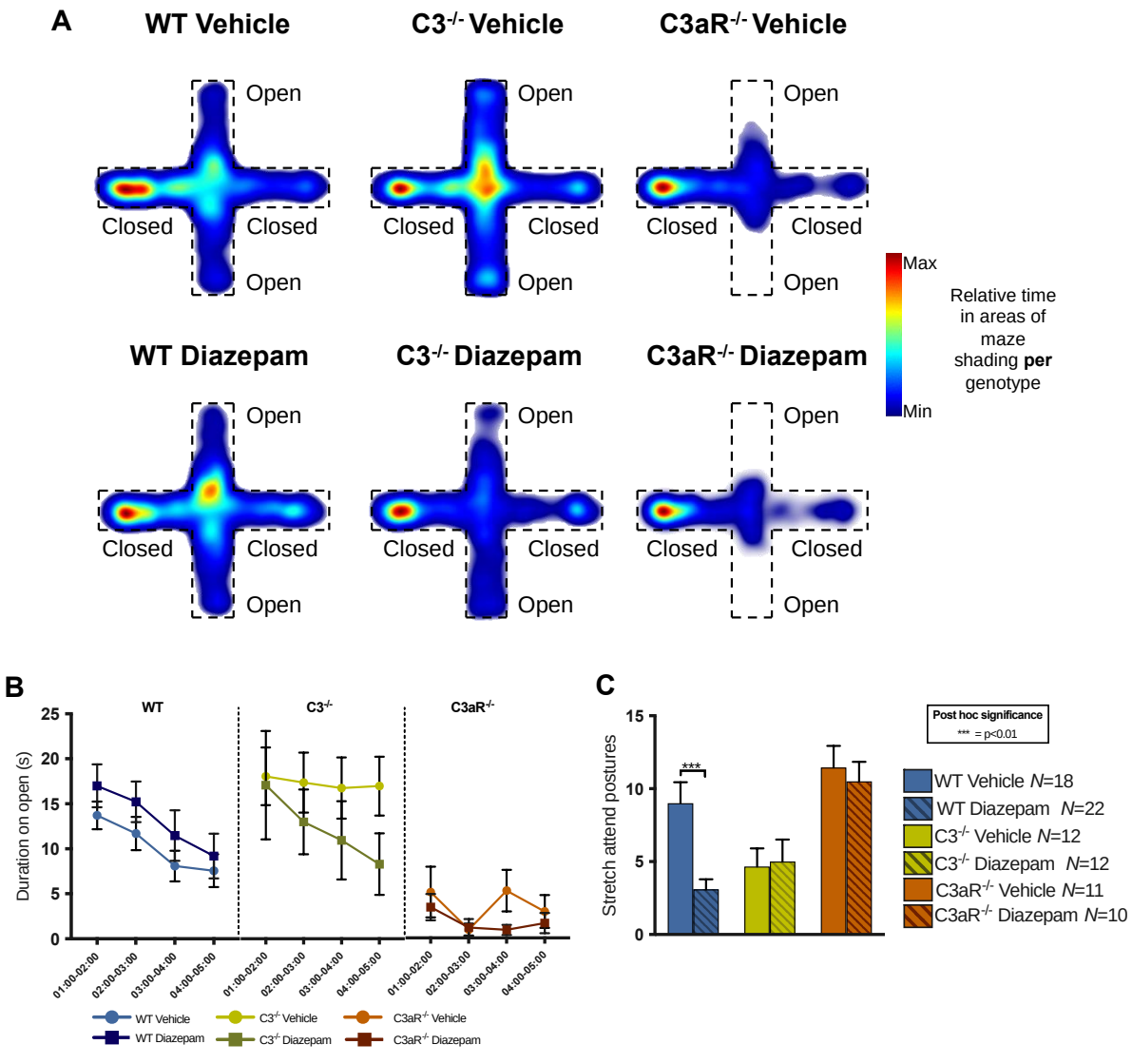

Figure 3. Altered sensitivity to diazepam in *C3aR*$^{-/-}$ and *C3*$^{-/-}$ mice. Behaviourally naïve mice were treated with either diazepam (2mg/kg, i.p) or vehicle injections once daily for 2 days and then 30 minutes prior to testing. (**A)** Heatmaps demonstrating duration spent in zones of the maze by vehicle treated and diazepam treated animals **(B)** Plots showing duration spent on open arms in 1-minute time bins (start-01:00 was excluded due to effect of diazepam in delaying initial entry to open arms across genotypes, see Supplementary Figure 4A). There was a trend for wildtype diazepam treated animals to spend more time on the open arms throughout the task although this did not reach significance (main effect of DRUG, $F_{1,38}$=1.41, p=0.2462). In *C3*$^{-/-}$ mice there was a strong tendency for drug treated animals to explore the open arms less than vehicle treated *C3*$^{-/-}$ mice (main effect of DRUG, $F_{1,22}$=1.25, p=0.2764). A similar, though less pronounced pattern was seen in *C3aR*$^{-/-}$ mice (main effect of DRUG, $F_{1,19}$=1.55, p=0.2284) **(C)** There were genotype differences in SAPs (main effect of GENOTYPE, $F_{2,79}$=10.7, p<0.0001), a main effect of DRUG ($F_{1,79}$=4.13, p=0.0454) and a significant GENOTYPE × DRUG interaction ($F_{2,79}$=4.64, p=0.0138). *Post hoc* tests showed that diazepam significantly reduced the number of SAPs in wildtype mice only (wildtype vehicle 9.00±1.44 vs. wildtype diazepam 3.09±0.71, p=0.0006, *C3*$^{-/-}$ vehicle 4.67±1.24 vs. *C3*$^{-/-}$ diazepam 5.00±1.51, p=0.9975, *C3aR*$^{-/-}$ vehicle 11.45±1.49 vs. *C3aR*$^{-/-}$ diazepam 10.50±1.34, p=0.9558). Data are mean + S.E.M. *** represents p≤0.001 for *post-hoc* genotype comparisons.

3.4 Enhanced fear learning in *C3*$^{-/-}$ but not *C3aR*$^{-/-}$ mice

Psychiatric disorders are associated with maladaptive responses to both innate and learned aversive stimuli[56,57]. We therefore extended our analysis to investigate whether the behavioural dissociations in innate anxiety observed between *C3*$^{-/-}$ and *C3aR*$^{-/-}$ mice would also apply to learned or conditioned fear, where a previously neutral cue generates a fear response as a result of predicting an aversive outcome. In a further group of male mice, we used the fear-potentiated startle (FPS) paradigm[30,58] a well-established method of generating learned fear responses to an acute and imminent danger signal that is characteristic of fear. In this paradigm (see Figure 4A and Methods Section 2.7) fear learning is indexed by an enhanced response to a startling noise in the presence of a cue (the conditioned stimulus or CS) previously paired with mild foot shock (the unconditioned stimulus). In the pre-conditioning session, pulse-alone trials revealed increased basal startle reactivity in both *C3aR*$^{-/-}$ and *C3*$^{-/-}$ mice relative to wildtype (Figure 4B). Increased reactivity to the unconditioned foot shock stimulus (in the absence of any startle stimulus) during the conditioning session was also observed in both knockouts (Figure 4C). However, these common effects of genotype were not seen in the fear-potentiated startle measures which index fear learning. Whilst all groups showed the expected enhancement of the startle response in the presence of the CS, the effect of the CS was significantly greater in *C3*$^{-/-}$ animals relative to the *C3aR*$^{-/-}$ and wildtype mice (Figure 4D), indicating enhanced learning of the fear related-cue by the *C3*$^{-/-}$ mice. This pattern of effects was also observed in female mice (Figure S8). This was the opposite pattern of effects to those observed in the tests of innate anxiety and showed a double dissociation in the impact of manipulating C3 and C3aR function that depended fundamentally on the nature of the aversive stimulus.

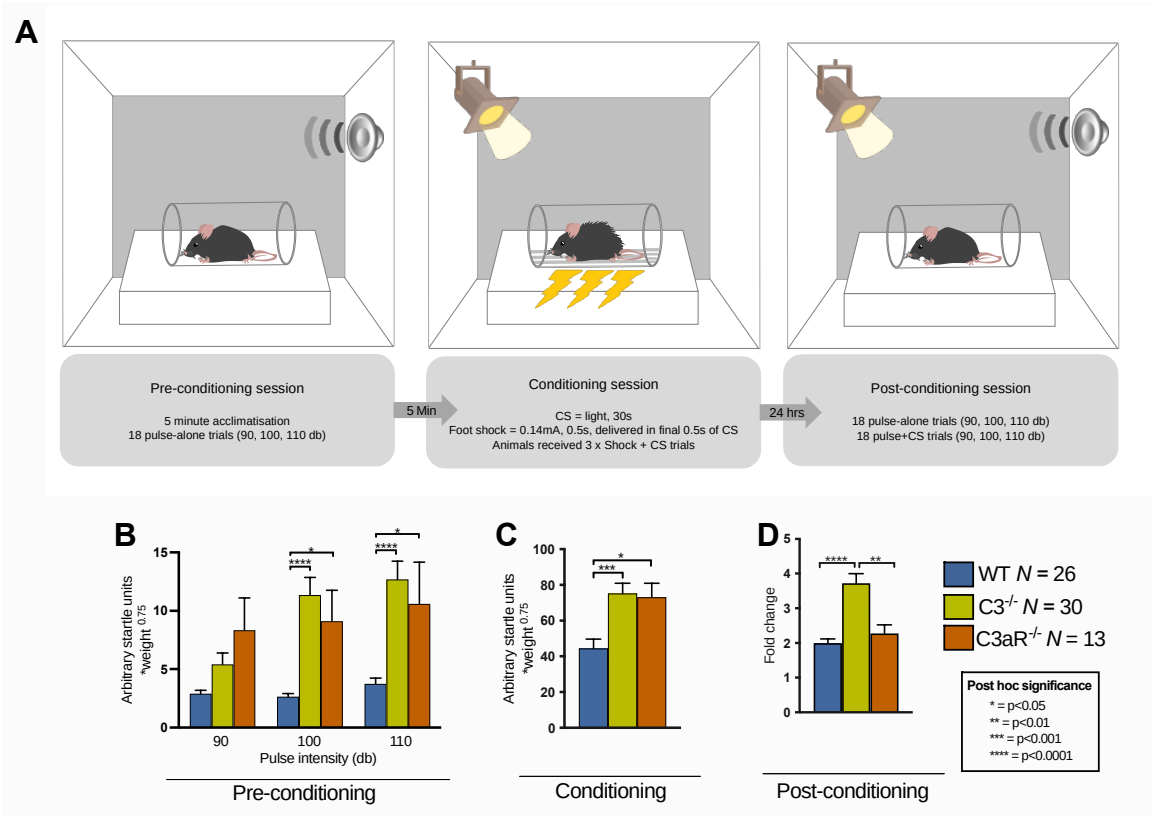

Figure 4. Enhanced fear-potentiated startle in *C3*$^{-/-}$ but not *C3aR*$^{-/-}$ mice. (A) Flow chart depicting the FPS protocol used, which took place in three separate sessions over two consecutive days. Baseline startle reactivity to a range of pulse intensities was assessed in the pre-conditioning session, immediately preceding the conditioning session in which a visual stimulus (light) was paired with 3 weak foot shocks. 24 hours later, subjects were re-introduced to the same chamber and startle reactivity was compared between pulse-alone trials and pulse+CS trials to determine the degree of FPS. On all trials, the peak startle response was recorded and normalised for body weight differences using Kleiber's 0.75 mass exponent, and fold-changes calculated. **(B)** There was a significant main effect of GENOTYPE ($F_{2,66}$=9.04, p=0.0003) and a significant GENOTYPE × STIMULUS INTENSITY interaction ($F_{4,132}$=7.55, p<0.0001). *C3*$^{-/-}$ and *C3aR*$^{-/-}$ mice demonstrated increased levels of startle responding relative to wildtype mice at 100dB (*C3*$^{-/-}$ 11.34±1.51 vs. wildtype 2.63±0.26, p<0.0001, *C3aR*$^{-/-}$ 9.12±2.63 vs. wildtype p=0.0174) and 110dB (*C3*$^{-/-}$ 12.69±1.55 vs. wildtype 3.74±0.50,

p<0.0001, *C3aR*$^{-/-}$ 10.58±3.58 vs. wildtype p=0.0111) **(C)** *C3*$^{-/-}$ and *C3aR*$^{-/-}$ mice also showed increased startle responding to the footshock+CS (*C3*$^{-/-}$ 75.18±5.73, *C3aR*$^{-/-}$ 73.14±7.78) pairings relative to wildtype mice (44.34±5.29, *C3*$^{-/-}$ vs. wildtype p=0.0006, *C3aR*$^{-/-}$ vs. wildtype p=0.0137, overall ANOVA $F_{2,66}$=8.7, p=0.0004), although it should be noted that responses were much greater to these stimuli in all mice than to the startle stimuli in the pre-conditioning session. **(D)** In the post-conditioning session, all mice demonstrated increases to the pulse+CS stimuli in comparison to pulse-alone stimuli, as demonstrated by the fold-change increase in startle responding, however, this effect was significantly increased in *C3*$^{-/-}$ mice (3.72±0.27) relative to wildtype (1.99±0.11, p<0.0001) and *C3aR*$^{-/-}$ mice (2.27±0.24, p=0.0056, overall Kruskal-Wallis test H_2=27.7, p<0.0001). Data are mean + S.E.M. *, **, *** and **** represent p≤0.05, p≤0.01, p≤0.001 and p≤0.0001 for *post-hoc* genotype comparisons, respectively.

3.5 Complement signalling pathways underlying abnormal learned fear phenotypes in *C3*$^{-/-}$ mice

Given the central role of C3 within the complement system, its deletion affects a number of distal pathways (Figure 5A), with the activity of the C3a/C3aR, C3b/CR3, C5a/C5aR and terminal pathways affected. Therefore, the loss of function of any of these pathways may have contributed to the observed fear learning phenotype in *C3*$^{-/-}$ mice. However, it is possible to exclude effects due to loss of the C3a/C3aR pathway since the fear learning phenotype was specific to *C3*$^{-/-}$ and not *C3aR*$^{-/-}$ mice (Figure 4D). This left iC3b/CR3 signalling and/or pathways downstream of C5 (i.e. C5a/C5aR, terminal pathway) as the remaining possibilities. In order to distinguish between these pathways, we repeated the FPS experiment with the addition of *C5*$^{-/-}$ mice. This model

has intact C3a/C3aR and iC3b/CR3 signalling, but lacks C5a/C5b and terminal pathway activity, as do *C3*$^{-/-}$ mice (Figure 5A). We hypothesised that if C*5*$^{-/-}$ mice also displayed enhanced fear-potentiated startle, then the phenotype in *C3*$^{-/-}$ mice would likely be due to a loss of C5a/C5aR signalling or the terminal pathway. On the other hand, if *C5*$^{-/-}$ mice demonstrated normal fear-potentiated startle, this would confine the likely mediating pathway in *C3*$^{-/-}$ mice to iC3b/CR3 signaling (Figure 5A).

Results from the pre-conditioning session demonstrated increases in the startle response of C*5*$^{-/-}$ mice, (Figure 5B) although in this instance the previously observed enhanced startle reactivity in C*3*$^{-/-}$ mice (Figure 4B) was not replicated. In the conditioning session, there was again evidence of increased startle responses to shock (Figure 5C) in C*3*$^{-/-}$ mice and responses were of a similar magnitude in C*5*$^{-/-}$ mice, although these were not significantly different to wildtype. We replicated the previous finding of enhanced fear-potentiated startle in *C3*$^{-/-}$ mice (Figure 5D), but critically both male (Figure 5) and female (Figure S9) *C5*$^{-/-}$ mice showed no evidence of enhanced fear learning and were comparable to wildtypes, indicating that loss of iC3b/CR3 signalling, but not loss of C5a/C5aR and the terminal pathway, was involved in the *C3*$^{-/-}$ fear learning phenotype. Additionally, we did not observe innate anxiety-like phenotypes in *C5*$^{-/-}$ male mice (Figure S5).

This pattern of effects allowed us to distinguish between the likely mechanisms underlying the enhanced learned fear in *C3*$^{-/-}$ mice, as we could exclude concomitant loss of C5a/C5aR signalling or molecules downstream of C5, and hence also exclude an explanation based on effects of C5a/C5aR signalling on developmental neurogenesis[59,60]. Instead, these data raised the possibility of an explanation based

on the established effects of the iC3b/CR3 pathway on synaptic pruning, a mechanism involving microglia mediated elimination of synapses impacting on neurodevelopment and learning-related synaptic plasticity[13,14,61].

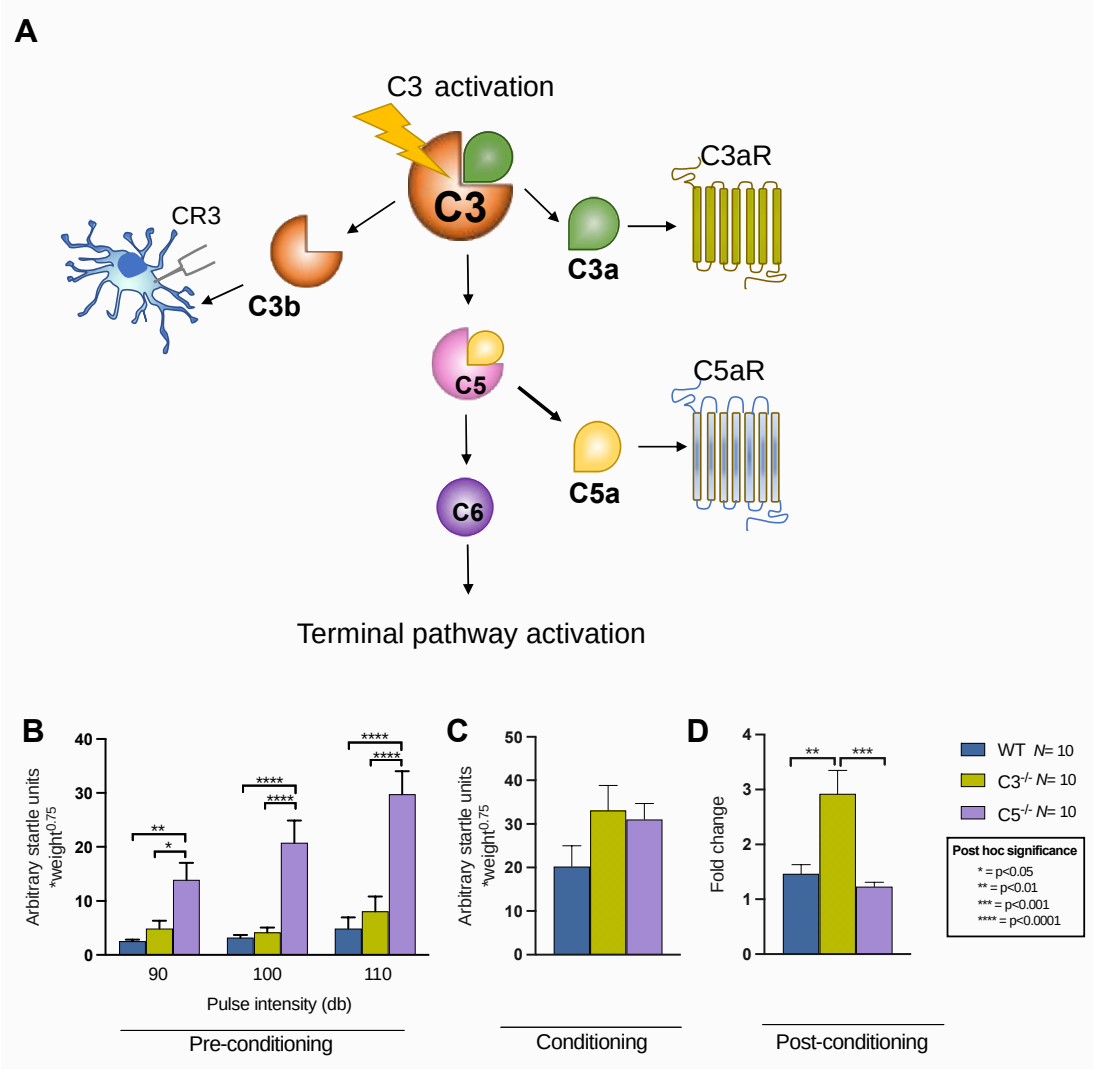

Figure 5. Pathways underlying fear learning phenotypes in *C3*$^{-/-}$ mice (A) C3 activation leads to generation of cleavage fragments C3a and C3b. The former signals via C3aR whereas the latter signals via complement receptor 3 (CR3). C3b is also necessary for forming the convertase enzyme that cleaves C5. Upon cleavage, C5 generates the fragments C5a and C5b (not shown). C5a signals via the C5aR, whereas C5b propagates activity of the terminal complement pathway via C6. Since

C3 cannot be activated in *C3*$^{-/-}$ mice, the action of all these pathways (C3a/C3aR, C3b/CR3, C5a/C5aR, terminal pathway) is absent. By using *C5*$^{-/-}$ mice, which lack C5a/C5aR and terminal pathway activity, we examined whether lack of C3b/CR3, C5a/C5aR or the terminal pathway was responsible for fear learning phenotypes in *C3*$^{-/-}$ mice. **(B)** In the pre-conditioning session there were significant main effects of GENOTYPE ($F_{2,27}$=18.4, p<0.0001) and STIMULUS INTENSITY ($F_{2,54}$=19.0, p<0.0001) and a significant GENOTYPE × STIMULUS INTENSITY interaction ($F_{4,54}$=7.00, p<0.0001). *C5*$^{-/-}$ mice demonstrated increased levels of startle responding relative to wildtype and *C3*$^{-/-}$ mice at all stimulus intensities (90dB; WT 2.55±0.26 vs. *C5*$^{-/-}$ 13.92±3.14, p=0.0069, *C3*$^{-/-}$ 4.92±1.40 vs. *C5*$^{-/-}$ p=0.0405, WT vs. *C3*$^{-/-}$ p=0.7919; 100dB; WT 3.23±0.45 vs. *C5*$^{-/-}$ 20.83±4.07, p<0.0001, *C3*$^{-/-}$ 4.924.17±0.88 vs. *C5*$^{-/-}$ p<0.0001, WT vs. *C3*$^{-/-}$ p=0.9639; 110dB; WT 4.92±2.03 vs. *C5*$^{-/-}$ 29.78±4.29, p<0.0001, *C3*$^{-/-}$ 8.07±2.76 vs. *C5*$^{-/-}$ p<0.0001, WT vs. *C3*$^{-/-}$ p=0.6643). **(C)** There were no significant differences in startle responses to the footshock+CS pairings during the conditioning session (WT 20.23±4.76, *C3*$^{-/-}$ 33.10±5.74, *C5*$^{-/-}$ 31.08±3.59, $F_{2,27}$=2.10, p=0.1421). **(D)** In the post-conditioning session, all mice demonstrated increases to the pulse+CS stimuli in comparison to pulse-alone stimuli, as demonstrated by the fold-change increase in startle responding, however, this effect was again significantly increased only in *C3*$^{-/-}$ mice (2.92±0.43) relative to wildtype (1.47±0.17, p=0.0020) and *C5*$^{-/-}$ mice (1.23±0.08, p=0.0004, overall ANOVA $F_{2,27}$=11.5, p=0.0002). Data represent mean + S.E.M. *, **, *** and **** represent p≤0.05, p≤0.01, p≤0.001 and p≤0.0001 for *post-hoc* genotype comparisons, respectively.

3.6 Differential expression of stress and anxiety related genes in *C3aR*$^{-/-}$ and *C3*$^{-/-}$ mice

We next sought to assess whether the dissociations in innate anxiety and learned fear between *C3aR*$^{-/-}$ and *C3*$^{-/-}$ models were associated with differential gene expression in brain regions associated with emotional behaviours. We assayed gene expression in male mice, within three regions of recognised importance in stress and anxiety; the medial prefrontal cortex (mPFC), ventral hippocampus (vHPC) and cerebellum[28,62](Figure 6A). Given our previous data showing differential corticosterone responses and altered sensitivity to diazepam in both knockouts, we first measured expression of the glucocorticoid receptor *Nr3c1* and the corticotrophin-releasing hormone receptor 1 *Crhr1*, together with *Gabra2* which encodes the $GABA_A$ receptor α2 subunit responsible for mediating benzodiazepine anxiolysis[63]. There were no effects of genotype on *Crhr1* and *Gabra2* mRNA expression in any of the brain regions assayed (Figure 6B,C). *Nr3c1* expression did however show effects of genotype with trends indicating increases in *C3aR*$^{-/-}$ mice in the mPFC and vHPC, and significantly increased expression in cerebellum that was common to both knockouts (Figure 6D).

As activation of C3aR has been shown to stimulate calcium influx from the extracellular space[2-4,64,65] and calcium channel subunit variants have strong links to risk for psychiatric and neurological disorders, as well as anxiety phenotypes[66,67], we also investigated a panel of voltage-gated calcium channels. Expression of *Cacna1d,* which encodes the Cav1.3 channel of L-type calcium gated voltage channels, was increased in the mPFC of *C3aR*$^{-/-}$ mice (Figure 6E) and in both *C3*$^{-/-}$ and *C3aR*$^{-/-}$ mice there was upregulation of cerebellar *Cacna1e,* which encodes the Cav2.3 channel of R-type voltage gated calcium channels (Figure 6F). We also investigated the expression of *Cacna1c* which encodes the $Ca_V1.2$ subunit of L-type voltage gated calcium channels

that forms the channel pore allowing calcium entry[68]. We found genotype and brain region specific changes in *Cacna1c* expression, with selective increases in expression in *C3aR*$^{-/-}$ mice in the vHPC and cerebellum, but not the mPFC (Figure 6G).

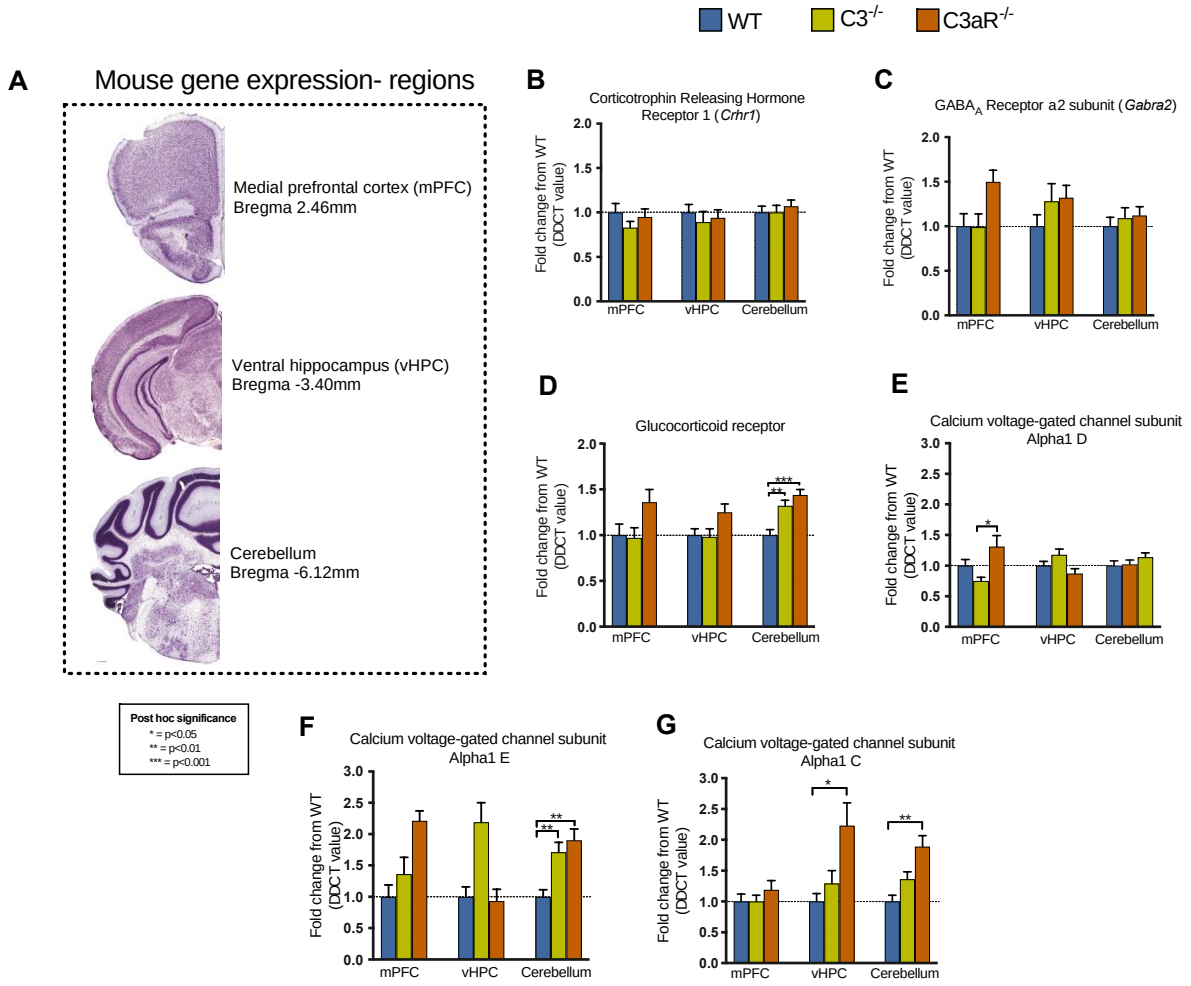

Figure 6. mRNA expression of stress and anxiety related genes. (A) Animals were culled and the medial prefrontal cortex (mPFC), ventral hippocampus (vHPC) and cerebellum were dissected. **(B)** There were no significant differences in the expression of Corticotrophin releasing hormone receptor 1 (*Crhr1*) in any region, across genotypes (mPFC $F_{2,53}$=0.587, p=0.5597, N wildtype=20, *C3*$^{-/-}$=17, *C3aR*$^{-/-}$= 19; vHPC $F_{2,49}$=0.169, p=0.8450, N WT=20, *C3*$^{-/-}$=15, *C3aR*$^{-/-}$= 17; cerebellum $F_{2,47}$=0.0482, p=0.8346, N WT=19, *C3*$^{-/-}$=17, *C3aR*$^{-/-}$= 14). **(C)** There were also no significant

changes in the expression of the $GABA_A$ receptor α2 subunit (*Gabra2*) in any region, across genotypes (mPFC H_2=1.04, p=0.5939, N wildtype=20, *C3*$^{-/-}$=19, *C3aR*$^{-/-}$= 16; vHPC $F_{2,49}$=0.721, p=0.4914, N WT=20, *C3*$^{-/-}$=13, *C3aR*$^{-/-}$= 19; cerebellum $F_{2,47}$=0.221, p=0.8026, N WT=18, *C3*$^{-/-}$=17, *C3aR*$^{-/-}$= 15). **(D)** Expression of the glucocorticoid receptor (*Nr3c1*) was significantly increased in the cerebellum of both *C3*$^{-/-}$ and *C3aR*$^{-/-}$ groups ($F_{2,61}$=10.3, p=0.0002, *C3*$^{-/-}$ vs. wildtype p=0.0023, *C3aR*$^{-/-}$ vs. wildtype p=0.0002, N wildtype=19, *C3*$^{-/-}$=20, *C3aR*$^{-/-}$= 15). There were trends towards increased expression of the glucocorticoid receptor gene *Nr3c1* in the mPFC and vHPC of *C3aR*$^{-/-}$ mice but these were not significant (mPFC; $F_{2,56}$=1.33, p=0.2723, N wildtype=20, *C3*$^{-/-}$=20, *C3aR*$^{-/-}$= 19, vHPC; $F_{2,62}$=1.11, p=0.3345, N wildtype=23, *C3*$^{-/-}$=20, *C3aR*$^{-/-}$= 22). **(E)** Calcium voltage-gated channel subunit Alpha 1d (*Cacna1d*) expression was changed in the mPFC ($F_{2,36}$=7.52, p=0.0407) owing to altered expression between *C3*$^{-/-}$ and *C3aR*$^{-/-}$ mice (p=0.0314; N wildtype=11, *C3*$^{-/-}$=13, *C3aR*$^{-/-}$= 15). There were no differences in the vHPC ($F_{2,31}$=2.27, p=0.1199, N wildtype=14, *C3*$^{-/-}$=10, *C3aR*$^{-/-}$= 10) or cerebellum ($F_{1,39}$=0.648, p=0.5286, N wildtype=14, *C3*$^{-/-}$=16, *C3aR*$^{-/-}$= 12). **(F)** Expression of the Calcium voltage-gated channel subunit Alpha 1e (*Cacna1e*) was significantly upregulated in the cerebellum of both knockouts ($F_{2,39}$=7.52, p=0.0017, wildtype vs. *C3*$^{-/-}$ p=0.0082, wildtype vs. *C3aR*$^{-/-}$ p=0.0032; N wildtype=14, *C3*$^{-/-}$=16, *C3aR*$^{-/-}$= 12). There were borderline significant changes in expression in the vHPC ($F_{2,32}$=3.15, p=0.0565, N wildtype=14, *C3*$^{-/-}$=11, *C3aR*$^{-/-}$= 10) and no significant changes in the mPFC (H_2=3.43, p=0.1802, N wildtype=11, *C3*$^{-/-}$=12, *C3aR*$^{-/-}$= 15).**(G)** Expression levels of the Calcium voltage-gated channel subunit Alpha 1c (*Cacna1c*) were significantly increased in *C3aR*$^{-/-}$ mice in a regionally specific manner in the vHPC ($F_{2,47}$=3.20, p=0.0496, *C3*$^{-/-}$ vs. wildtype p=0.6895, *C3aR*$^{-/-}$ vs. wildtype p=0.0295, N wildtype=21, *C3*$^{-/-}$=13, *C3aR*$^{-/-}$= 16) and the cerebellum

($F_{2,54}$=5.84, p=0.0051, *C3*$^{-/-}$ vs. wildtype p=0.1613, *C3aR*$^{-/-}$ vs. wildtype p=0.0024, N wildtype=20, *C3*$^{-/-}$=20, *C3aR*$^{-/-}$= 17). There were no significant changes in the mPFC ($F_{2,52}$=1.04, p=0.5939, N wildtype=20, *C3*$^{-/-}$=19, *C3aR*$^{-/-}$= 16). Data represent fold change from wildtype + SEM. *, **, *** represent p≤0.05, p≤0.01 and p≤0.001 for *post-hoc* genotype comparisons, respectively.

4. Discussion

Using knockout models manipulating specific complement proteins, we have revealed dissociable effects of complement pathways on distinct elements of aversive behaviours. *C3aR*$^{-/-}$ mice displayed a profound innate anxiety phenotype that was lacking in *C3*$^{-/-}$ mice. The specificity of the anxiety phenotype exhibited by *C3aR*$^{-/-}$ mice at the behavioural level was paralleled by EPM-evoked corticosterone levels, confirming the validity of the EPM as an index of anxiety-like behaviour. In contrast, when we examined learned fear, where a previously neutral cue generates a fear response as a result of predicting an aversive outcome, we found that the dissociation was reversed with the *C3*$^{-/-}$ mice exhibiting an enhanced fear response to a conditioned cue, but no differences between wildtype and *C3aR*$^{-/-}$mice. These findings indicate that closely related elements of the complement system can differentially impact upon the neural mechanisms underlying innate anxiety and learned fear, pointing to a hitherto unrecognized complexity of complement effects on brain function and behaviour of relevance to emotional dysfunction in psychopathology.

Our findings extend previous findings of abnormal anxiety behaviour in *C3aR*$^{-/-}$ mice[35]. Our use of specific complement knockout models allowed us to further pinpoint the

likely complement pathways and potential mechanisms underlying C3aR-mediated anxiety. Since C3a is solely produced via C3 cleavage, and C3aR is the canonical receptor for C3a, we hypothesised that any phenotypes dependent on the binding of C3a to the C3aR would be apparent in both *C3*$^{-/-}$ and *C3aR*$^{-/-}$ models. However, this was not borne out in our data. Given the divergence in phenotypes seen, one explanation is that the *C3aR*$^{-/-}$ anxiety phenotypes are independent of C3a and instead mediated by an alternative ligand. It has long been speculated that there may be promiscuity of the C3aR due to its unusually large second extracellular loop[69]. Indeed, a cleavage fragment of the neuropeptide precursor protein VGF (non-acronymic), TLQP-21, was recently reported to bind the C3aR[70,71]. This peptide has pleiotropic roles including in the stress response[72] and its precursor VGF is widely expressed throughout the CNS[73] and in regions associated with stress reactivity such as the hypothalamus, where there is evidence for C3aR expression[74,75]. Determining whether the mechanisms underlying innate anxiety phenotypes in *C3aR*$^{-/-}$ mice are dependent on TLQP-21/C3aR interactions will be a priority for future work.

Whether the *C3aR*$^{-/-}$ phenotypes described here are the result of ongoing effects of *C3aR* deletion in the adult brain or instead the enduring consequence of neurodevelopmental impacts of *C3aR* deficiency also remains to be determined. On the basis of previous findings implicating C3aR in both developmental neurogenesis[76] and in acute brain changes following behavioural manipulations[77], both are possibilities. One strategy would be to test whether acute administration of the C3aR antagonist SB290157[78] phenocopies the constitutive knockout of *C3aR*, though at present no data is available on the CNS penetration of SB290157 and this molecule has received criticism due to evidence of agonist activity[79].

Interestingly, recent preclinical work has suggested a protective role for C3a/C3aR in chronic-stress induced depressive-behaviour[91]. Given the common co-occurrence of anxiety and depression, our findings of enhanced anxiety in *C3aR*$^{-/-}$ mice might seem at odds with the reported resilience of this strain^{-} to depression-related phenotypes[91]. However, the chronic unpredictable-stress paradigm used in these studies is likely to evoke significant inflammation, and therefore the extent to which our data in acutely stressed animals can be compared is questionable. Our corticosterone data indicated that whilst *C3aR*$^{-/-}$ mice had greater reactivity in after a 5-minute exposure to the EPM, their stress levels were normal at baseline. Further studies are thus needed to determine how the anxiety phenotype of *C3aR*$^{-/-}$ mice may be modulated by stressors of a more chronic nature, and also whether dissociations may also exist in the impact of the C3aR on depressive and anxiety-like behaviours.

We also probed mechanisms underpinning the *C3aR*$^{-/-}$ innate anxiety phenotype by assessing the effects of the anxiolytic drug diazepam. We found that a dose of diazepam that was anxiolytic in wildtype mice had no effect in *C3aR*$^{-/-}$ mice. Stretch attend postures, thought to reflect risk assessment behaviour[54], are highly sensitive to pharmacological manipulation[50,80] and in agreement with our own findings, diazepam has been shown to specifically decrease SAPs in the absence of effects on open arm exploration[81]. Importantly, *C3aR*$^{-/-}$ mice consistently performed more SAPs than other genotypes, and therefore floor effects cannot account for the pattern of results observed. Benzodiazepines act on $GABA_A$ receptors[63] however we found no significant changes in expression of *Gabra2*, a $GABA_A$ receptor subunit responsible for anxiolytic actions of benzodiazepines in tests of innate anxiety[63], in the brain

regions sampled. This raises the possibility of alternative molecular mechanisms mediating the anxiety phenotypes seen in the *C3aR*$^{-/-}$ model. Whatever the molecular underpinnings of the dissociable anxiety phenotypes, our data show a profoundly altered effect of diazepam in both knockouts; a lack of response in *C3aR*$^{-/-}$ and an apparent paradoxical anxiogenic effect of the drug in *C3*$^{-/-}$ mice, though this interpretation needs to take into account an apparent selective sedative effect in *C3*$^{-/-}$ mice.

In contrast to innate anxiety, we observed a specific effect of *C3* knockout on conditioned fear. The absence of a comparable phenotype in *C3aR*$^{-/-}$ and *C5*$^{-/-}$ mice suggested that these effects were unlikely to be due to loss of either C3a/C3aR, C5a/C5aR, or the terminal pathway, and instead that enhanced fear learning phenotypes in *C3*$^{-/-}$ mice were likely dependent on loss of the iC3b/CR3 pathway. This pathway has been strongly implicated in activity dependent synaptic elimination during neurodevelopment[13,25] and in age-dependent synapse loss[82]. While demonstrations of complement mediated synaptic pruning during development have centered on the visual system, complement-mediated microglial phagocytosis of dopamine D1 receptors has been demonstrated in the nucleus accumbens with functional impacts on social behaviour[83]. It remains to be seen whether complement mediated processes of this nature, within brain regions linked to fear processing such as the ventral hippocampus, amygdala and prefrontal cortex are responsible for enhanced fear learning in *C3*$^{-/-}$ mice, or whether this phenotype is a general consequence of altered synaptic elimination throughout the *C3*$^{-/-}$ brain. In addition to developmental processes, the iC3b/CR3 pathway could also be involved acutely in fear learning. *C3* mRNA is upregulated during discrete stages of fear learning[77] and microglial CR3 is implicated

771 in long term depression[84]. Furthermore, complement-mediated engulfment of
772 synapses by microglia may be important in the forgetting of fear memories[14].
773
774 At the gene expression level, we found some changes which were common to both
775 knockouts, and one result that was specific to *C3aR*$^{-/-}$ mice. Regarding the latter, there
776 was a highly specific increase in expression of *Cacna1c* in the ventral hippocampus
777 and cerebellum of *C3aR*$^{-/-}$ mice. This finding is of potential interest given the strong
778 evidence implicating *CACNA1C* variants in genetic risk for a broad spectrum of
779 psychiatric disorders including schizophrenia and bipolar disorder[66], with anxiety
780 phenotypes reported in both human risk variant carriers[85] and animal models[86-89].
781 Furthermore, recent evidence indicates convergent polygenic mechanisms shared
782 between complement and other psychiatric risk genes[90], including calcium regulation
783 pathways, and thus our study lends further support to an interaction between these
784 systems. Whether alterations in *Cacna1c* are of direct functional relevance to the
785 *C3aR*$^{-/-}$ anxiety phenotypes observed here remains to be determined experimentally.
786 We also observed increased cerebellar expression of the glucocorticoid receptor in
787 both *C3*$^{-/-}$ and *C3aR*$^{-/-}$ mice, suggesting that these alterations may result from the
788 absence of C3a/C3aR signalling. Expression of these genes did not differentiate
789 between models and therefore were unlikely to contribute to the dissociable effects of
790 the knockouts on behaviour and stress hormone physiology. Future studies of
791 neuronal activity in brain regions linked to emotion may be more informative in terms
792 of functional neuroanatomy underlying the anxiety-related behavioural and
793 physiological differences seen in the knockout models.
794

In summary, our study provides an in-depth behavioural phenotyping of complement knockout models revealing distinct effects of complement signaling pathways on emotional behaviours relating to fear and anxiety. These findings add significantly to the evidence that perturbations of the complement system, whether reduced complement activation as in the present work or excessive activation as is predicted by *C4* genetic variants[24,92], have major and dissociable effects on brain and behavioural phenotypes of relevance to core clinical symptoms of psychiatric disease.

5. Author's contributions

The study was designed by LJW, TH, BPM, WPG and LSW. LJW and TH performed behavioural experiments with assistance from NH. Molecular analyses were performed by SAB, EB, MT, ALM, AIB and LJW. Data interpretation were carried out by JH, MJO, JR, WPG, NH, TRH, BPM, LSW and TH. The manuscript was drafted by LJW, TH, WPG and LSW. All authors approved the final manuscript.

6. Acknowledgements

The authors thank Professor Craig Gerard and Professor Marina Botto for provision of the *C3aR*$^{-/-}$ and *C5*$^{-/-}$ strains respectively, and to Rhys Perry, Pat Mason, Helen Read and other staff at Cardiff University BIOSV for their invaluable animal care and husbandry. This work was supported by a Wellcome Trust Integrative Neuroscience PhD Studentship awarded to LJW (099816/Z/12/Z), a Waterloo Foundation Early Career Fellowship awarded to LJW, a Hodge Centre for Neuropsychiatric Immunology Seed Corn and Project grant awarded to LJW and a Wellcome Trust Strategic Award 100202/Z/12/Z (DEFINE) held by the Neuroscience and Mental Health Research Institute at Cardiff University (LSW and JH).

7. Competing financial interests

The authors declare no competing financial interests.

8. Materials and correspondence

All data from this study are available from the corresponding authors upon reasonable request.

9. References

1. Coulthard, L. G. & Woodruff, T. M. Is the Complement Activation Product C3a a Proinflammatory Molecule? Re-evaluating the Evidence and the Myth. *J. Immunol.* **194,** 3542–3548 (2015).
2. Norgauer, J. *et al.* Complement fragment C3a stimulates Ca2+ influx in neutrophils via a pertussis-toxin-sensitive G protein. *Eur. J. Biochem.* **217,** 289–294 (1993).
3. Möller, T., Nolte, C., Burger, R., Verkhratsky, A. & Kettenmann, H. Mechanisms of C5a and C3a Complement Fragment-Induced [Ca2+]i Signaling in Mouse Microglia. *Journal of Neuroscience* **17,** 615–624 (1997).
4. Lian, H., Li, Y., Lu, H.-C. & Zheng, H. NFκB-Activated Astroglial Release of Complement C3 Compromises Neuronal Morphology and Function Associated with Alzheimer's Disease. **85,** 101–115 (2015).
5. Sayah, S. *et al.* Two different transduction pathways are activated by C3a and C5a anaphylatoxins on astrocytes. *Molecular Brain Research* **112,** 53–60 (2003).
6. Morley, B. J. & Walport, M. J. *The Complement FactsBook*. (Academic Press, 1999).
7. Kemper, C. & Köhl, J. Back to the future – non-canonical functions of complement. *Seminars in Immunology* **37,** 1–3 (2018).
8. Nataf, S., Stahel, P. F., Davoust, N. & Barnum, S. R. Complement anaphylatoxin receptors on neurons: new tricks for old receptors? *Trends Neurosci.* **22,** 397–402 (1999).
9. Veerhuis, R., Nielsen, H. M. & Tenner, A. J. Complement in the brain. *Molecular Immunology* **48,** 1592–1603 (2011).
10. Bénard, M., Gonzalez, B. J., Biological, M. S. J. O.2004. Characterization of C3a and C5a receptors in rat cerebellar granule neurons during maturation neuroprotective effect of C5a against apoptotic cell death. *J Biol. Chem,* **42***,* 43487-43496 (2004).
11. Rahpeymai, Y. *et al.* Complement: a novel factor in basal and ischemia-induced neurogenesis. *EMBO J* **25,** 1364–1374 (2006).
12. Gorelik, A. *et al.* Developmental activities of the complement pathway in migrating neurons. *Nature Communications* **8,** 15096 (2017).

13. Stevens, B. *et al.* The classical complement cascade mediates CNS synapse elimination. *Cell* **131,** 1164–1178 (2007).
14. Wang, C. *et al.* Microglia mediate forgetting via complement-dependent synaptic elimination. *Science,* **367,** 688-694 (2020).
15. Harold, D. *et al.* Genome-wide association study identifies variants at CLU and PICALM associated with Alzheimer's disease. *Nature Genetics* **41,** 1088–1093 (2009).
16. Jansen, I. E. *et al.* Genome-wide meta-analysis identifies new loci and functional pathways influencing Alzheimer's disease risk. *Nature Genetics* **51**, 404–413 (2019).
17. Shi, Q. *et al.* Complement C3-Deficient Mice Fail to Display Age-Related Hippocampal Decline. *Journal of Neuroscience* **35,** 13029–13042 (2015).
18. Zhou, J., Fonseca, M. I., Pisalyaput, K. & Tenner, A. J. Complement C3 and C4 expression in C1q sufficient and deficient mouse models of Alzheimer's disease. *Journal of Neurochemistry* **106,** 2080–2092 (2008).
19. Corbett, B. A. *et al.* A proteomic study of serum from children with autism showing differential expression of apolipoproteins and complement proteins. *Mol. Psychiatry* **12,** 292 (2007).
20. Maes, M., Delange, J., Ranjan, R., Meltzer, H. Y. & Desnyer, R. Acute phase proteins in schizophrenia, mania and major depression: modulation by psychotropic drugs. *Pharmacology Biochemistry and Behaviour* 1–11 (1997). doi:10.1016/S0165-1781(96)02915-0
21. Ruland, T. *et al.* Molecular serum signature of treatment resistant depression. *Psychopharmacology* 1–9 (2016).
22. Song, Y. R. *et al.* Specific alterations in plasma proteins during depressed, manic, and euthymic states of bipolar disorder. *Brazilian Journal of Medical and Biological Research* **48,** 973–982
23. Oganesyan, L. P., Mkrtchyan, G. M., Sukiasyan, S. H. & Boyajyan, A. S. Classic and alternative complement cascades in post-traumatic stress disorder. *Bull. Exp. Biol. Med.* **148,** 859–861 (2009).
24. Sekar, A. *et al.* Schizophrenia risk from complex variation of complement component 4. *Nature, **530,*** 117–183 (2016).
25. Schafer, D. P. *et al.* Microglia Sculpt Postnatal Neural Circuits in an Activity and Complement-Dependent Manner. *Neuron* **74,** 691–705 (2012).
26. Håvik, B. *et al.* The Complement Control-Related Genes CSMD1 and CSMD2 Associate to Schizophrenia. *BPS* **70,** 35–42 (2011).
27. Zhang, S. *et al.* Association Between Polymorphisms of the Complement 3 Gene and Schizophrenia in a Han Chinese Population. *Cell. Physiol. Biochem.* **46,** 2480–2486 (2018).
28. Tovote, P., Fadok, J. P. & Lüthi, A. Neuronal circuits for fear and anxiety. *Nat. Rev.* **16,** 317–331 (2015).
29. Perusini, J. N. & Fanselow, M. S. Neurobehavioral perspectives on the distinction between fear and anxiety. *Learn. Mem.* **22,** 417–425 (2015).
30. Davis, M. Neural systems involved in fear and anxiety measured with fear-potentiated startle. *Am Psychol* **61,** 741–756 (2006).
31. Engin, E. *et al.* Modulation of anxiety and fear via distinct intrahippocampal circuits. . *eLife,* **5:e14120**, (2016).

32. Yilmaz, M. *et al.* Overexpression of schizophrenia susceptibility factor human complement C4A promotes excessive synaptic loss and behavioral changes in mice. *Nat Neurosci* 1–31 (2020).
33. Girardi, G. *et al.* Imaging of activated complement using ultrasmall superparamagnetic iron oxide particles (USPIO)-conjugated vectors: An in vivo in utero non-invasive method to predict placental insufficiency and abnormal fetal brain development. *Mol. Psychiatry* **20,** 1017–1026 (2015).
34. Kulkarni, A. P., Govender, D. A., Kotwal, G. J. & Kellaway, L. A. Modulation of anxiety behavior by intranasally administered Vaccinia virus complement control protein and curcumin in a mouse model of Alzheimer's disease. *Current Alzheimer Research* **8,** 95–113 (2011).
35. Pozo-Rodrigálvarez, A., Ollaranta, R., Skoog, J., Pekny, M. & Pekna, M. Hyperactive Behavior and Altered Brain Morphology in Adult Complement C3a Receptor Deficient Mice. *Front. Immunol.* **12,** 604812 (2021).
36. Fischer, M. B., Ma, M., Goerg, S., Zhou, X. & Xia, J. Regulation of the B cell response to T-dependent antigens by classical pathway complement. *J.Immunol,* **157,** 549-556, (1996).
37. Humbles, A. A. *et al*. A role for the C3a anaphylatoxin receptor in the effector phase of asthma. *Nature,* **406,** 998–1001 (2000).
38. Wang, Y. *et al.* A role for complement in antibody-mediated inflammation: C5-deficient DBA/1 mice are resistant to collagen-induced arthritis. *J. Immunol.* **164,** 4340–4347 (2000).
39. Mikaelsson, M. A., ncia, M. C. A., Dent, C. L., Wilkinson, L. S. & Humby, T. Placental programming of anxiety in adulthood revealed by Igf2-null models. *Nature Communications* **4,** 1–9 (2013).
40. Molewijk, H. E., van der Poel, A. M. & Olivier, B. The ambivalent behaviour 'stretched approach posture' in the rat as a paradigm to characterize anxiolytic drugs. *Psychopharmacology* **121,** 81–90
41. Mackintosh, J. H. & Grant, E. C. A Comparison of the Social Postures of Some Common Laboratory Rodents. *Behaviour* **21,** 246–259 (1963).
42. Kleiber, M. Body size and metabolism. *Hilgardia Journal of Agricultural Science* **6,** 315–353 (1932).
43. Mikaelsson, M. A., Constância, M., Dent, C. L., Wilkinson, L. S. & Humby, T. Placental programming of anxiety in adulthood revealed by Igf2-null models. *Nature Communications* **4,** 2311 (2013).
44. Dickmeis, T. Glucocorticoids and the circadian clock. *Journal of Endocrinology* **200,** 3–22 (2008).
45. Livak, K. J. & Schmittgen, T. D. Analysis of Relative Gene Expression Data Using Real-Time Quantitative PCR and the 2−ΔΔCT Method. *Methods* **25,** 402–408 (2001).
46. Wright, S. P. Adjusted p-values for simultaneous inference. *Biometrics* **48,** 1005–1013 (1992).
47. Pellow, S., Chopin, P., File, S. E. & Briley, M. Validation of open : closed arm entries in an elevated plus-maze as a measure of anxiety in the rat. *J. Neurosci. Methods* **14,** 149–167 (1985).
48. Walf, A. A. & Frye, C. A. The use of the elevated plus maze as an assay of anxiety-related behavior in rodents. *Nat Protoc* **2,** 322–328 (2007).
49. Ennaceur, A. Tests of unconditioned anxiety - pitfalls and disappointments. *Physiology & Behavior* **135,** 55–71 (2014).

50. RODGERS, R. J. Anxiety, defence and the elevated plus-maze. *Pharmacology Biochemistry and Behaviour* (1997).
51. Braun, A. A., Skelton, M. R., Vorhees, C. V. & Williams, M. T. Comparison of the elevated plus and elevated zero mazes in treated and untreated male Sprague-Dawley rats: Effects of anxiolytic and anxiogenic agents. *Pharmacology Biochemistry and Behavior* **97,** 406–415 (2011).
52. Lepicard, E. M., Joubert, C., Hagneau, I., Perez-Diaz, F. & Chapouthier, G. Differences in anxiety-related behavior and response to diazepam in BALB/cByJ and C57BL/6J strains of mice. *Pharmacology Biochemistry and Behavior* **67,** 739–748 (2000).
53. Grewal, S. S., Sherperd, D, J. K., Bill, D. J., Fletcher, A. & Dourish, C. T. Behavioural and pharmacological characterisation of the canopy stretched attend posture test as a model of anxiety in mice and rats. *Psychopharmacology* **133,** 29–38 (1997).
54. Kaesermann, H. P. Stretched attend posture, a non-social form of ambivalence, is sensitive to a conflict-reducing drug action. *Psychopharmacology* **89,** 31–37
55. Albrechet-Souza, L., Cristina de Carvalho, M., Rodrigues Franci, C. & Brandão, M. L. Increases in plasma corticosterone and stretched-attend postures in rats naive and previously exposed to the elevated plus-maze are sensitive to the anxiolytic-like effects of midazolam. *Hormones and Behavior* **52,** 267–273 (2007).
56. Holt, D. J., Coombs, G., Zeidan, M. A., Goff, D. C. & Milad, M. R. Failure of neural responses to safety cues in schizophrenia. *Arch Gen Psychiatry* **69,** 893–903 (2012).
57. Grillon, C., Morgan, C. A., Southwick, S. M., Davis, M. & Charney, D. S. Baseline startle amplitude and prepulse inhibition in Vietnam veterans with posttraumatic stress disorder. *Psychiatry Research* **64,** 169–178 (1996).
58. Falls, W. A., Carlson, S., Turner, J. G. & Willott, J. F. Fear-potentiated startle in two strains of inbred mice. *Behavioral Neuroscience* **111,** 855–861 (1997).
59. Coulthard, L. G. *et al.* Complement C5aR1 Signaling Promotes Polarization and Proliferation of Embryonic Neural Progenitor Cells through PKCζ. *J. Neurosci.* **37,** 5395–5407 (2017).
60. Hawksworth, O. A., Coulthard, L. G., Taylor, S. M., Wolvetang, E. J. & Woodruff, T. M. Brief Report: Complement C5a Promotes Human Embryonic Stem Cell Pluripotency in the Absence of FGF2. *Stem Cells,* **32,** 3278-3284, (2014).
61. Schafer, D. P. *et al.* Microglia sculpt postnatal neural circuits in an activity and complement-dependent manner. *Neuron* **74,** 691–705 (2012).
62. Apps, R. & Strata, P. Neuronal circuits for fear and anxiety - the missing link. *Nat. Rev.* **16,** 642 (2015).
63. Smith, K. S., Engin, E., Meloni, E. G. & Rudolph, U. Benzodiazepine-induced anxiolysis and reduction of conditioned fear are mediated by distinct GABAA receptor subtypes in mice. *Neuropharmacology* **63,** 250–258 (2012).
64. Ahamed, J., Venkatesha, R. T., Thangam, E. B. & Ali, H. C3a Enhances Nerve Growth Factor-Induced NFAT Activation and Chemokine

Production in a Human Mast Cell Line, HMC-1. *J. Immunol.* **172,** 6961–6968 (2004).

65. Wu, F. *et al.* Complement component C3a plays a critical role in endothelial activation and leukocyte recruitment into the brain. *J Neuroinflammation* **13,** 23 (2016).
66. Hamshere, M. L. *et al.* Genome-wide significant associations in schizophrenia to ITIH3/4, CACNA1C and SDCCAG8, and extensive replication of associations reported by the Schizophrenia PGC. *Mol. Psychiatry* 1–5 (2019).
67. Kabir, Z. D. *et al.* Rescue of impaired sociability and anxiety-like behavior in adult cacna1c-deficient mice by pharmacologically targeting eIF2α. *Mol. Psychiatry* **22,** 1096–1109 (2017).
68. Simms, B. A. & Zamponi, G. W. Neuronal Voltage-Gated Calcium Channels: Structure, Function, and Dysfunction. *Neuron* **82,** 24–45 (2014).
69. Chao, T. H. *et al.* Role of the second extracellular loop of human C3a receptor in agonist binding and receptor function. *Journal of Biological Chemistry* **274,** 9721–9728 (1999).
70. Hannedouche, S. *et al.* Identification of the C3a Receptor (C3AR1) as the Target of the VGF-derived Peptide TLQP-21 in Rodent Cells. *Journal of Biological Chemistry* **288,** 27434–27443 (2013).
71. Cero, C. *et al.* The TLQP-21 peptide activates the G-protein-coupled receptor C3aR1 via a folding-upon-binding mechanism. *Structure* **22,** 1744–1753 (2014).
72. Razzoli, M. *et al.* Implication of the VGF-derived peptide TLQP-21 in mouse acute and chronic stress responses. *Behav. Brain Res.* **229,** 333–339 (2012).
73. van den Pol, A. N., Bina, K., Decavel, C. & Ghosh, P. VGF expression in the brain. *J. Comp. Neurol.* **347,** 455–469 (1994).
74. Lewis, B., Francis, K., Gasque, P., Scanlon, M. & Ham, J. Functional complement C3a receptors in the rat pituitary gland. *Endocrine Abstracts* **3,** 198 (2002).
75. Francis, K. Complement C3a receptors in the pituitary gland: a novel pathway by which an innate immune molecule releases hormones involved in the control of inflammation. *The FASEB Journal* 1–4 (2003).
76. Coulthard, L. G., Hawksworth, O. A. & Woodruff, T. M. Complement: The Emerging Architect of the Developing Brain. *Trends Neurosci.* **41,** 373–384 (2018).
77. Scholz, B. *et al.* The Regulation of Cytokine Networks in Hippocampal CA1 Differentiates Extinction from Those Required for the Maintenance of Contextual Fear Memory after Recall. *PLoS ONE* **11,** e0153102–29 (2016).
78. Ames, R. S. *et al.* Identification of a selective nonpeptide antagonist of the anaphylatoxin C3a receptor that demonstrates anti-inflammatory activity in animal models. *J. Immunol.* **166,** 6341–6348 (2001).
79. Therien, A. G., Baelder, R. & Köhl, J. Agonist Activity of the Small Molecule C3aR Ligand SB 290157. *J. Immunol.* **174,** 7479–7480 (2005).
80. Holly, K. S., Orndorff, C. O. & Murray, T. A. MATSAP: An automated analysis of stretch-attend posture in rodent behavioral experiments. *Scientific Reports* **6,** (2016).

81. Genewsky, A. *et al.* How much fear is in anxiety? BioRxiv preprint doi:10.1101/385823
82. Hong, S. *et al.* Complement and microglia mediate early synapse loss in Alzheimer mouse models. *Science* **352,** 712–716 (2016).
83. Kopec, A. M., Smith, C. J., Ayre, N. R., Sweat, S. C. & Bilbo, S. D. Microglial dopamine receptor elimination defines sex-specific nucleus accumbens development and social behavior in adolescent rats. *Nature Communications* **9,** 3769 (2018).
84. Zhang, J. *et al.* Microglial CR3 Activation Triggers Long-Term Synaptic Depression in the Hippocampus via NADPH Oxidase. *Neuron* **82,** 195–207 (2014).
85. Roussos, P., Giakoumaki, S. G., Georgakopoulos, A., Robakis, N. K. & Bitsios, P. The CACNA1C and ANK3 risk alleles impact on affective personality traits and startle reactivity but not on cognition or gating in healthy males. *Bipolar Disorders* **13,** 250–259 (2011).
86. Bader, P. L. *et al.* Mouse model of Timothy syndrome recapitulates triad of autistic traits. *Proc. Natl. Acad. Sci. U.S.A.* **108,** 15432–15437 (2011).
87. Lee, A. S. *et al.* Forebrain elimination of cacna1c mediates anxiety-like behavior in mice. *Nat.Neurosci* **17,** 1054–1055 (2012).
88. Dao, D. T. *et al.* Mood Disorder Susceptibility Gene CACNA1C Modifies Mood-Related Behaviors in Mice and Interacts with Sex to Influence Behavior in Mice and Diagnosis in Humans. *Biological Psychiatry* **68,** 801–810 (2010).
89. Dedic, N. *et al.* Cross-disorder risk gene CACNA1C differentially modulates susceptibility to psychiatric disorders during development and adulthood. *Nat.Neurosci* **23,** 533–543 (2018).
90. Kim, M. *et al.* Brain gene co-expression networks link complement signaling with convergent synaptic pathology in schizophrenia. *Nat Neurosci* **24,** 799–809 (2021).
91. Crider, A. *et al.* Complement component 3a receptor deficiency attenuates chronic stress-induced monocyte infiltration and depressive-like behavior. *Brain, Behavior, and Immunity* **70,** 246–256 (2018).
92. Sellgren, C. M. *et al.* Increased synapse elimination by microglia in schizophrenia patient-derived models of synaptic pruning. *Nat.Neurosci* **22,** 1–385 (2019).